

The Synergy of Damage Repair and Retention Promotes Rejuvenation and Prolongs Healthy Lifespans in Cell Lineages

Barbara Schnitzer¹, Johannes Borgqvist¹, Marija Cvijovic^{1*}

¹ Department of Mathematical Sciences, University of Gothenburg, Sweden

* corresponding author: Marija Cvijovic, marija.cvijovic@chalmers.se

Abstract

Damaged proteins are inherited asymmetrically during cell division in the yeast *Saccharomyces cerevisiae*, such that most damage is retained within the mother cell. The consequence is an ageing mother and a rejuvenated daughter cell with full replicative potential. Daughters of old and damaged mothers are however born with increasing levels of damage resulting in lowered replicative lifespans. Remarkably, these prematurely old daughters can give rise to rejuvenated cells with low damage levels and recovered lifespans, called second-degree rejuvenation. We aimed to investigate how damage repair and retention together can promote rejuvenation and at the same time ensure low damage levels in mother cells, reflected in longer health spans. We developed a dynamic model for damage accumulation over successive divisions in individual cells as part of a dynamically growing cell lineage. With detailed knowledge about single-cell dynamics and relationships between all cells in the lineage we can infer how individual damage repair and retention strategies affect the propagation of damage in the population. We show that active damage retention lowers damage levels in the population by reducing the variability across the lineage, and results in larger population sizes. Repairing damage efficiently in early life, as opposed to investing in repair when damage has already accumulated, counteracts accelerated ageing caused by damage retention. It prolongs the health span of individual cells which are moreover less prone to stress. In combination, damage retention and early investment in repair are beneficial for healthy ageing in yeast cell populations.

Keywords : *damage accumulation, replicative ageing, healthy ageing, yeast*

Introduction

Even to this day, a conceptual understanding of ageing as a phenomenon is lacking [1, 2]. Accordingly, the task of explaining the origins of specific symptoms of ageing on an organism level beginning from molecular processes in a single cell is highly complicated, and the first step in achieving this goal is to properly define the term. One of the most feasible theories on the origins of ageing, the disposable soma theory [3], states that in circumstances with limited resources an organism will prioritise reproduction over maintenance of the body, called the soma, referred to as a division of labour [4]. Further, its occurrence is motivated by the observation that, in nature, most animals die at a young age due to various factors such as starvation or predation [1], and therefore natural selection will favour genes resulting in rapid growth followed by reproduction as opposed to traits associated with longevity. Thus, the expected consequence of the removal of such factors leading to death is the degradation of the soma since the germ cells are prioritised. To investigate the precise molecular properties of this degradation, it is advantageous to examine the division of labour in less complex biological systems.

The unicellular predecessor of this process can be studied in the budding yeast *Saccharomyces cerevisiae* (*S.cerevisiae*). Here, the division of labour occurs on the population level between the larger mother cells, corresponding to the soma, and the smaller daughter cells, corresponding to the germ line [5]. In particular, the ageing process in yeast is characterised by an increase in both size and generation time, as well as an accumulation of different types of damage called ageing factors. One of the most universal ageing factors are misfolded or oxidatively damaged proteins [6]. Although the cell has developed intracellular responses to the formation of detrimental byproducts, such as the repair and degradation of damage by an extensive protein quality control system [7–10], these processes are imperfect and under these conditions the accumulation of damage is inevitable [11, 12].

A population level response to the accumulated damage in order to ensure the generation of viable daughter cells is the asymmetric distribution of damage between the progenitor and progeny after cell division. This entails that the mother sacrifices herself by preventing damage from leaking over to the daughter [13]. This asymmetry is a crucial component of ageing, motivated by the fact that it is a conserved mechanism which has been found in species ranging from bacteria to mammals, and in particular it is found in human stem cells [14–22]. The process is essential for maintaining the viability of a population of cells [3, 23–25] by producing rejuvenated daughter cells [6, 26–28]. Simultaneously, over successive divisions damage will accumulate in the progenitor cell which eventually leads to the loss of its fitness and fecundity, i.e. replicative ageing,

which can ultimately be measured by the number of produced daughter cells over the course of its lifetime. Even though individual mother cells are disadvantaged, it ensures full replicative potential of the progeny and thereby the immortality of the lineage.

Since the budding yeast *S.cerevisiae* exhibits an asymmetric cell division, it has become a successful model organism to investigate replicative ageing [29–32]. Besides pure size asymmetry, several studies in yeast point to the existence of an active transport mechanism, called retention, which during cell division selectively segregates damaged cellular components within the mother cell compartment and reinforces rejuvenation [13, 27, 33–35]. However, in the late stages of the lifespan of a single mother cell rejuvenation becomes less effective and ageing factors are increasingly passed on to the daughters, which have a decreased replicative potential and, thus, are born prematurely old [36, 37]. Nevertheless, when these prematurely old cells start to proliferate their own daughters, i.e. cells in the second generation, are recovered back to full replicative potential and show an absence of ageing biomarkers, which is called second-degree rejuvenation [36]. To study the impact of these fundamental processes on the ageing process in the context of the disposable soma theory, a population level focus is required.

Together, the repair and retention of damage steer the ageing of individual cells ultimately affecting the well-being of the entire population, but the exact impact of these forces are not understood. To investigate this, single-cell data is not sufficient and information about progenitors is required additionally. Despite advances in experimental techniques, it is not possible experimentally to track all mother and daughter cells in a population over several generations and to gather information about explicit mother-daughter relations. To cope with the vast numbers of cells in a population, replicative ageing due to damage accumulation has therefore been successfully studied by means of simulations. In that way, the evolutionary benefit of rejuvenation caused by asymmetric cell division has been confirmed [23, 38]. Moreover, using mathematical modelling it was proposed that a more asymmetrical distribution caused by active retention of damage is advantageous as a means to cope with high damage formation rates, i.e. stress, and this increases the population fitness [39–41]. Also, an age-dependent maximal degree of retention has been suggested [42]. More recent modelling studies highlight the importance of the repair machinery in replicative ageing, since asymmetric damage distribution at cell division alone cannot eliminate damage from the system [43, 44]. However, existing studies have shown the benefit of asymmetric cell division for the population fitness through rejuvenation by measuring average population-based behaviour as the only indicator which entails that the heterogeneity of individual cells in the lineage has been neglected. Typically, the growth rate of the population or its size is considered, but in order to understand the precise underlying mechanisms of how the fitness is increased, properties of

individual cells in the lineage have to be considered.

Accordingly, the connection between the capacity of the repair or retention machinery of individual heterogeneous cells and population level properties, such as the distribution of damage or the overall fitness, remains unclear. To this end, the aim is to investigate the effect of altering the intracellular processes related to ageing of individual cells on features of the population as a whole.

Results

From a single-cell to a whole population model of replicative ageing

To investigate how ageing of the individual cells contributes to the overall behaviour of the entire population, we developed a dynamic model that is capable of simulating single-cell replicative ageing and its effect on cell populations.

Single cell model: The single cell model of damage accumulation builds on our replicative ageing model [42], describing the dynamics of functional ($P(t)$) and damaged (malfunctioning) $D(t)$ proteins over time. In the model presented here, the protein content evolves non-linearly depending on cell growth (g), the resilience to damage (Q), the damage formation rate (k_1), the damage repair rate (k_2) and a repair capacity (R) (Fig 1A). We introduced the repair capacity that allows to investigate the effect of accumulated damage on the repair machinery:

$$r(D) = k_2 R \sin \left[\frac{D(t)}{R} \right] \quad (1)$$

By setting bounds on $P(t) \in [0, 1]$, $D(t) \in [0, 1]$ and $R \in [\pi^{-1}, \infty]$ maximally half a period of the sine function is captured (see SI S2 for details). The repair capacity R tunes how much the repair declines with increasing accumulated damage D . For small amounts of damage the expression $r(D)$ is the same for all values of R . In particular, the rate of repair in that regime corresponds to damage repair rate k_2 . However, the profiles differ increasingly as the cell is ageing (Fig 2, repair term in sub-panel). Cells divide if the amount of functional proteins has reached a critical threshold $P(t) = 1$. At cell division the protein content is distributed between the mother and the new-born daughter cell according to their size proportion (s) and damage retention (re) (Fig 1A) and is based on the principle of mass conservation over generations [39, 42].

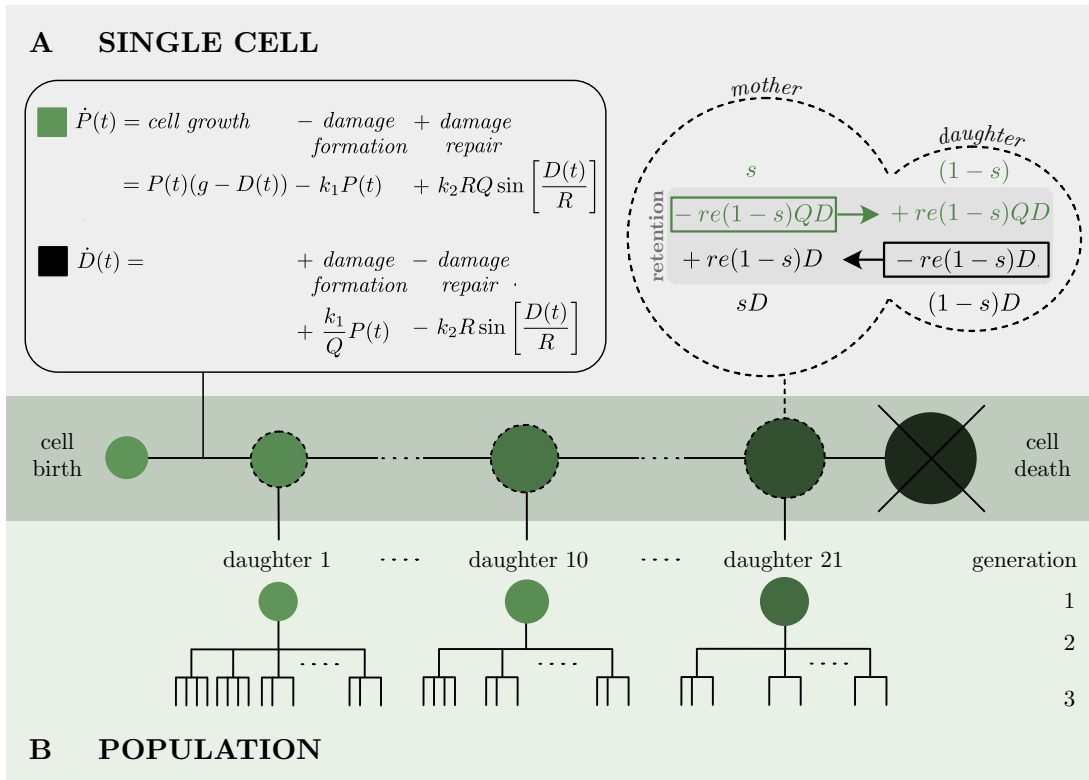


Figure 1: Schematic view of the model. **(A)** Left: Damage accumulation model of single-cells is governed by cell growth, damage formation and damage repair. Right: distribution of intact (green) and damaged (black) protein content between mother and daughter cell at division according to the size proportion s and the retention factor re . **(B)** Transition to the population model. Each cell division leads to a new-born daughter cell following an independent single-cell model, such that the lineage tree is recursively built up.

For simplicity, we assume s and re to be constant over the lifespan of a cell. In the model, we further assume full availability of nutrients at any time such that the total protein amount in the cell grows over time. However, damaged proteins slow down growth and, depending on the repair capacity, also damage repair. In combination with asymmetric damage segregation at cell division, we can simulate damage accumulation in mother cells that leads to the loss of fertility, thus replicative ageing. Subsequently, the cell is considered death when $D(t) = 1$. Both cell division and cell death are modelled as instantaneous events. The presented replicative ageing model of an individual cell is non-dimensionalised, resulting in the simpler model structure with a reduced number of parameters, simplifying the analysis of the system (SI S1).

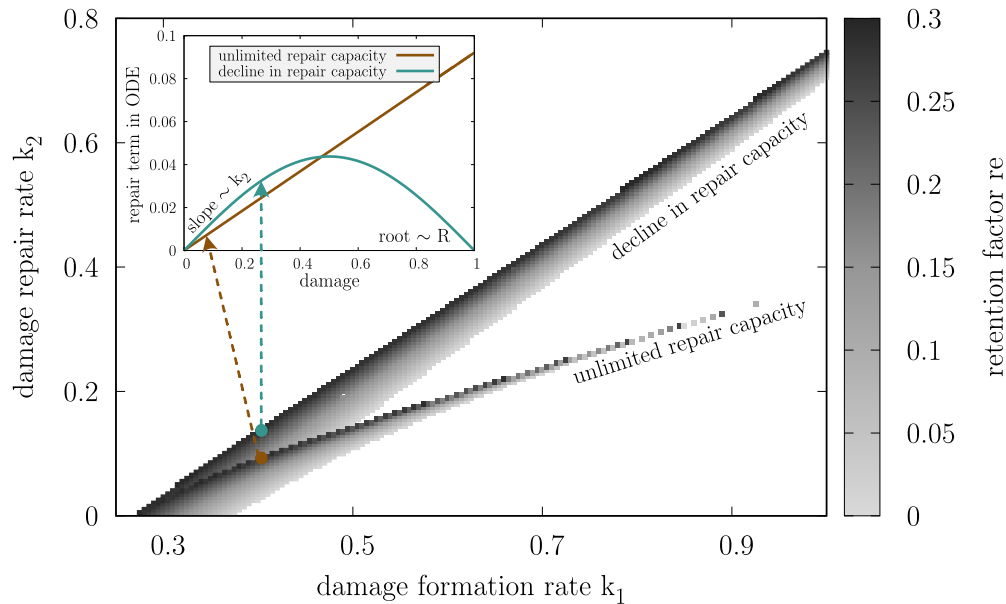


Figure 2: Discretised parameter combinations of damage formation rate (k_1), damage repair rate (k_2) and retention rate (re) leading to a constant replicative lifespan of 24 of initially damage-free cells for two distinct cases of repair capacity (R): unlimited repair capacity ($R \rightarrow \infty$) and decline in repair capacity ($R = \pi^{-1}$). The parameter space is divided into a grid with $\Delta k_1 = \Delta k_2 = 0.005$ and re is adapted accordingly (SI S3.3). The sub-panel shows exemplary repair rate profiles for constant $k_1 = 0.4$ and $re = 0.2957$.

Population model: From the single-cell model, we recursively build up the lineage by including all new-born cells in the population framework (Fig 1B) with explicit knowledge about all mother-daughter relations. After birth, each cell follows its own independent single-cell model that is initialised according to the distribution of proteins at cell division. We account for the individuality of cells by a non-linear mixed effect approach which has been shown to be a powerful tool to include cell-to-cell variability in population analysis [45]. Consequently, in our model the damage formation rate (k_1) and the damage repair rate (k_2) are drawn from a distribution with a population mean \bar{k}_1 and \bar{k}_2 and standard deviation $\sigma_1 = \sigma_2 = \sigma$, instead of being constant for all cells. To ensure positivity of the parameters a log-normal distribution was used. Each new cell has therefore a unique set of parameters.

$$k_1 = \bar{k}_1 \exp[\eta_1], \quad k_2 = \bar{k}_2 \exp[\eta_2], \quad \eta_1, \eta_2 \sim \mathcal{N}(0, \sigma^2) \quad (2)$$

All other parameters are specific to a certain population and do not vary across its individuals.

P(t), D(t) represent the content of functional P , damaged D proteins in the cell over time. $P(t_0)$ and $D(t_0)$ correspond to the protein content at the cell's birth.

S(t) represents the size of the cell $S(t) = P(t) + QD(t)$ over time. The size at cell birth is $S(t_0)$.

Lifetime represents the time from cell birth to cell death, $t_d - t_0$.

Replicative lifespan rls represents the total number of produced daughter cells before senescence.

Generation time represents the time between two successive divisions, $t_n - t_{n-1}$ for $n \in \{1, \dots, rls\}$.

Growth per cell cycle represents the relative size increase between two successive divisions, $\frac{S(t_n)}{S(t_{n-1})}$ for $n \in \{1, \dots, rls\}$.

Cumulative growth represents the relative total size increase during the lifetime, $\frac{S(t_d)}{S(t_0)}$.

Lineage position represents the relationship to the cell's ancestors up to the most recent common ancestor of the population (founder cell) represented by a set of indices $\{i, j, \dots\}$. The cell is the i^{th} daughter of its mother which is the j^{th} daughter of its own mother and so on.

Generation represents the level in the pedigree the cell is in with respect to the most recent common ancestor of the population (founder cell), equivalent to the cardinality of the lineage position.

Rejuvenation index rej represents the cell's degree of rejuvenation by $\frac{\Delta rls}{rls}$, with Δrls being the difference between the cell's replicative lifespan and its mother's replicative lifespan, and \bar{rls} being the average replicative lifespan in the population. A rejuvenated cells has $rej > 0$.

Health span h represents the fraction of the cell's lifespan where damage levels are below a critical threshold $D_c = D(t_c)$, defined by $\frac{t_c - t_0}{t_d - t_0} \cdot \frac{rls_c}{rls}$. t_c is defined as the time when the cell reaches D_c for the first time, while rls_c counts the number of divisions until this point. $h \in [0, 1]$. Large values of h correspond to a long health span.

Box 1: Single-cell properties.

In the course of this work we introduced a formal measure of rejuvenation (rejuvenation index) as the difference between the cell's and its mother's replicative lifespan scaled by the average replicative lifespan of the population, and a formal measure of health (health span) as the fraction of the cell's lifespan when

damage levels are below a given threshold coupled with the number of divisions accomplished until this time point.

For the dynamically growing yeast lineage, numerous properties of each individual cell and the whole cell population are defined and extracted. Individual cells are characterised by: replicative lifespan, rejuvenation index, health span, generation time, growth per cell cycle, cumulative growth, lifetime, lineage position and generation (Box 1), while the entire population is described by: population size, fraction of rejuvenated cells, fraction of healthy cells and population growth rate (Box 2). Additionally, distributions of all single-cell properties over the lineage can be studied.

Population size represents the amount of cells born in the lineage up to a certain generation.

Fraction of rejuvenated cells represents the the percentage of all cells in the population with a rejuvenation index $rej > 0$.

Fraction of healthy cells represents the percentage of all cells in the population with a health span $h > h_c$.

Growth rate represents how fast the population is growing in the exponential phase.

Box 2: Population properties.

In previous studies repair or degradation of damage is typically modelled as linear [39, 40, 42] or saturating functions of the present damage, inspired by Michaelis-Menten kinetics [43, 44]. In the study presented here, linear, saturated and declining profiles can be generated by changing the repair capacity R . Two distinct cases of the repair capacity are considered: unlimited repair capacity, corresponding to a constant rate of repair independent of the damage levels in the cell, and decline in repair capacity, corresponding to a continuous effect of damaged components on the repair machinery, especially evident towards the end of the cell's life where the effective rate of repair drops to zero. Intermediate values of R were investigated but do not add to the conclusions of this paper.

The proposed framework results in a detailed entire cell population model, including all intermediate branches and their explicate relationship, allowing to systematically infer how proposed repair and retention strategies of individual cells alter the propagation of damage in the pedigree and affect cellular rejuvenation and health spans.

Single-cell replicative ageing is steered by the synergy of damage repair and retention

To investigate how damage formation (k_1), damage repair (k_2), the repair capacity (R) and the retention factor (re) contribute to the replicative age of an individual cell, a discrete grid of parameter combinations leading to an average *wildtype* yeast lifespan of 24 divisions [46] was generated for two distinct repair mechanisms: unlimited repair capacity and decline in repair capacity (Fig 2).

Since higher damage formation rates and lower repair capacities are deleterious for the cells, they have to be compensated by either a faster repair or lower damage retention or both together to maintain the replicative lifespan. At the same time, decline in repair capacity corresponds to a decreasing functionality of damage repair when damage levels are high. In order to reach the same number of divisions the cell has to compensate with a more efficient repair when damage levels are low (Fig 2, repair term in sub-panel), reflected in generally higher values of repair rate k_2 . Decline in repair capacity leads to increased robustness as more parameter combinations, especially for large damage formation rates, yield the corresponding *wildtype* replicative lifespan. This result suggests that repair is especially important in the beginning of a cell's life when damage levels are low.

For qualitative comparison of repair and retention strategies and their effect on the population, we implemented the parameter grid as a starting point for the analysis. Considering that it is not sufficient to tune only one model parameter while keeping other parameters constant, since this immediately alters the replicative lifespan of all cells, at least two parameters have to be adapted according to the simulated parameter combinations.

Retention leads to bigger populations with lower damage levels

To investigate the effect of active damage retention on replicative ageing of the individual cell and the overall population behaviour, *wildtype* yeast populations with different retention factors (Fig 3) were simulated. The population parameters are chosen according to the previously described grid, where the damage formation rate remained constant, while the repair rate, repair capacity and retention were adapted accordingly. Due to the introduced cell-to-cell variability, respective damage formation and repair rates correspond to the population mean.

We found that independent of the repair mechanism, an increase in damage retention leads to larger populations (Fig 3A) with on average lower damage levels at birth (Fig 3A). We further investigated how damage propagates further over successive cell divisions in the population without and with active damage retention mechanism (Fig 3B). The results show that, independent of the re-

pair capacity, retention lowers the damage at birth in daughters regardless of the replicative age and damage levels of the mother cell (Fig 3B). While after successive divisions damage accumulates much faster in mothers that retain damage, during few early divisions both the damage in the mother and the daughter cells stay below corresponding levels of cells that do not retain damage, resulting in generally lower damage levels in the population.

We observed that decline in repair capacity generally leads to slightly decreased damage levels at birth compared to unlimited repair capacity (mean damage at birth is reduced by 3% when retention is not present to 20% with active damage retention) (Fig 3A), caused by slower damage accumulation in mother cells (Fig 3B).

Retention decreases the variability of the replicative lifespan across the lineage

To understand why populations consisting of cells with an active damage retention mechanisms are larger compared to those without, we analysed the cell lineages focusing on four cases: retention and no retention combined with decline in repair capacity and unlimited repair capacity. Cells were grouped according to the relation to their grandmother, corresponding to the the first two indices of their lineage position i and j . The cell is the i^{th} daughter of its mother which is in turn the j^{th} daughter of the its own mother (see Box 1 for details).

Without an active retention mechanism the population is highly diverse and the replicative age of the mother and even the grandmother at respective cell divisions have great influence on the lifespan of each cell (Fig 4, replicative lifespan). Mostly daughters of young mothers and grandmothers, corresponding to small i and j , are able to maintain the replicative lifespan. Daughters of old mothers, i.e. with large i , have a substantial disadvantage. In many cases they can only divide few times. Active damage segregation by retention decreases this variability and leads to lifespans around the typical value of *wildtype* cells across the pedigree. All branches in the lineage can quickly recover to full replicative potential such that the whole population can get larger. The repair capacity has in general no influence on the replicative lifespans for a given retention factor.

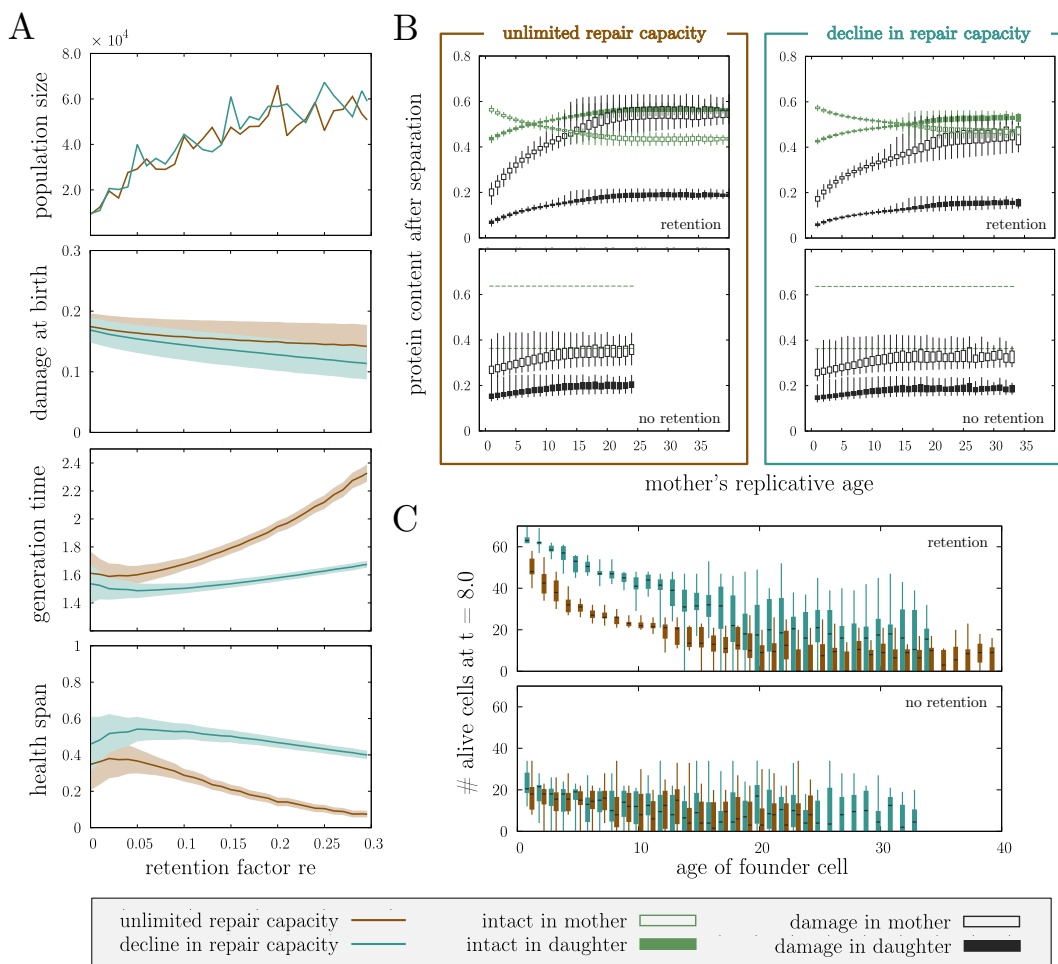


Figure 3: (A) Population size and mean and standard deviation of single-cell properties in *wildtype* cell lineages for varying retention factors re . Each population is initialised with 5 independent founder cells with average initial conditions and parameters according to SI S3. (B) Protein content in mother and daughter cell at division depending on the replicative age of the mother cell. No retention ($re = 0.0$) corresponds to 64% of the damage in the mother, while retention ($re = 0.2957$) corresponds to 74% of damage in the mother. The boxplots include the whole respective populations that were initialised by 10 independent founder cells with average initial conditions according to SI S3. (C) Number of cells at a specific early time point ($t = 8.0$ in dimensionless time) as an indication of the growth rate of the population in the exponential phase. Each boxplot reflects the statistics of 20 populations starting with one founder cell with average initial conditions and parameters according to SI S3.

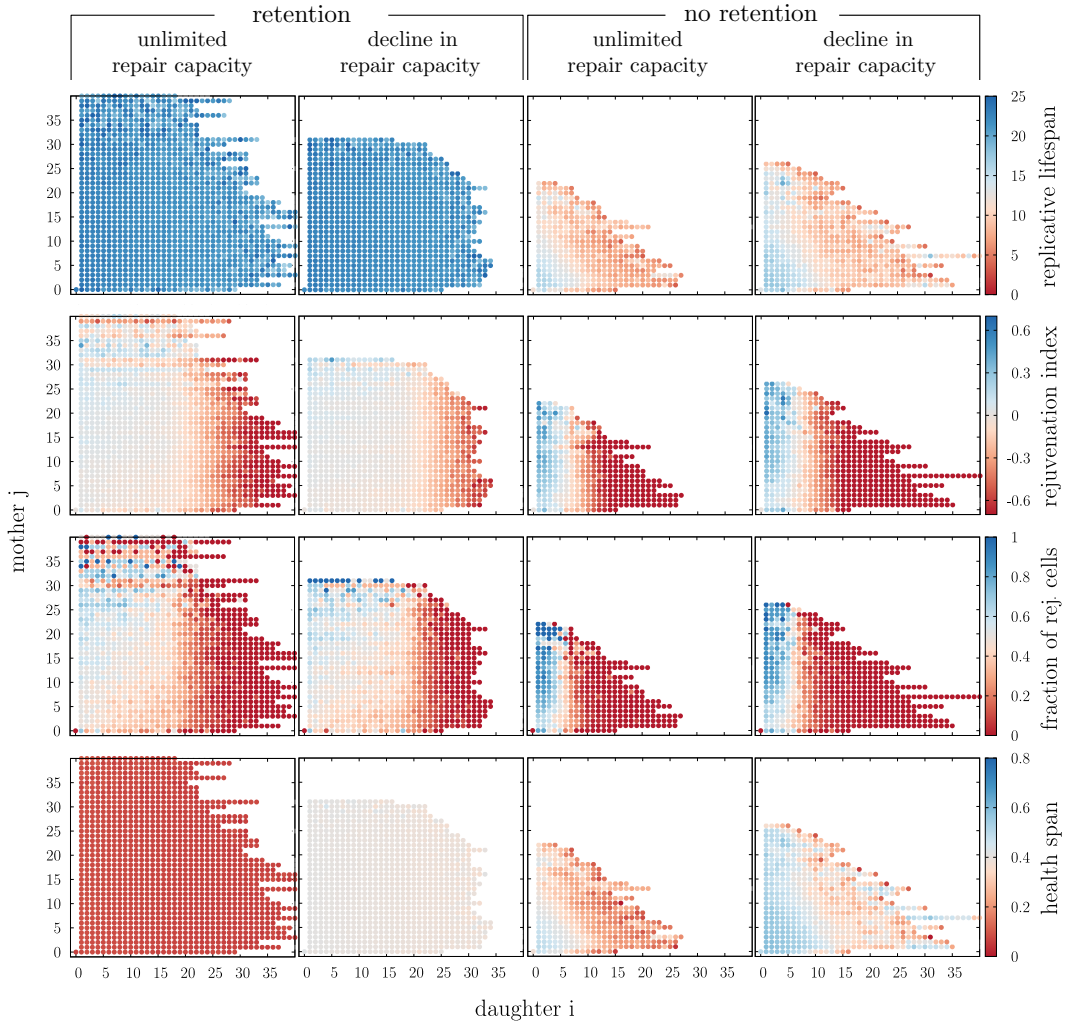


Figure 4: Mean or fraction of single-cell properties for *wildtype* cells that are grouped according to their lineage position with respect to the grandmother (indices i and j in lineage position). Each population is initialised with 10 independent founder cells with average initial conditions and parameters according to SI S3.

Decline in repair capacity results in lower damage levels and prolonged health spans by shortening generation times

The repair capacity profile has an effect on the damage levels in the population, without altering the replicative lifespans. To investigate this mechanisms, properties like generation times and health spans in individual cells were considered (Fig 3A).

Unlimited repair capacity leads on average to increased generation times and

decreased health spans in the populations when damage retention is increased. This is expected since damage retention loads the mother cell with extra damage. For decline in repair capacity these alterations are however only minor such that independent of retention average generation times are generally short and health spans long. For both repair profiles, the variability is decreased by retention.

This is further confirmed when health span (Fig 4) and generation time (Fig S4) were analysed with respect to the lineage position in the population. Both properties are more uniformly distributed across the lineage with retention. Even though there are also cells with very long health span and short generation times without retention, they are restricted to be born from young mothers and grandmothers. The same observation was previously made for the replicative lifespan.

Cells with decline in repair capacity efficiently repair damage in early divisions and have therefore short generation times. As a consequence, damage accumulates slower over successive divisions in mother cells after birth (Fig 3A) leading to longer health spans. Damage is diluted faster over the progeny and daughter cells are smaller at birth (Fig S4). Since the repair is highly affected by damage, it will quickly lose its functionality when damage takes over. Only then damage accumulates fast and proliferation is stopped rapidly. In contrast, unlimited repair capacity leads to faster damage accumulation in mother cells during early divisions and increasing generation times. Yet, cells can cope with damage better towards late divisions. They are able to divide even when already old and thus damaged, resulting in more daughter cells which are born prematurely old.

As already noted, the overall population size is not affected by the repair capacity (Fig 3A), however a fast populations growth in the exponential phase is influenced by decline in repair capacity leading to higher growth rates of the population due to decreased generation times, regardless of the age of the founder cell (Fig 3C).

Retention promotes rejuvenation across the cell lineage independent of the repair capacity

We further asked how rejuvenation is affected by retention and repair. We investigated rejuvenation indices across the pedigree for the simulated populations. In particular, we were interested in cells with positive rejuvenation index, i.e. daughters with a longer replicative lifespan compared to their mothers. We observed that rejuvenation occurs independent of the degree of retention and the repair capacity, purely caused by the asymmetry in size at division. Nonetheless, we found that active damage retention changes the distribution of rejuvenation across the pedigree for both repair capacities (Fig 4).

Due to the large variability in the lifespans without retention, we found ex-

tremely high absolute values of the rejuvenation index in these populations. Rejuvenated cells are however concentrated on specific parts of the lineage: only the first few daughters ($i \leq 5$) have the potential to rejuvenate. If these daughters are from mothers that are born prematurely old, i.e. coming from an old grandmother (large j), the daughters nearly certainly rejuvenate and in addition exhibit a large rejuvenation index (Fig 4, rejuvenation index and fraction of rejuvenated cells). Yet, it is a smaller fraction of the whole population that can rejuvenate (Fig S3) since later daughters ($i > 5$) have almost no chance to rejuvenate.

As previously described, large variability in replicative lifespans, as observed without retention, are hardly found with retention. As a consequence, rejuvenation becomes much more moderate but instead spreads over a larger part of the lineage (Fig 4, rejuvenation index and fraction of rejuvenated cells). Rejuvenation is no longer concentrated on the few early born daughters and up to the first 20 daughters of a cell have a significant chance to rejuvenate. Consequently, the total fraction of rejuvenated cells in the whole population increases compared to purely size dependent segregation of damage.

Characterisation of rejuvenated cells in the population

To characterise rejuvenated cells further apart from the lineage position, we investigated if they differ in other properties from cells that do not rejuvenate. Our simulated lineages revealed that rejuvenated cells are a small subset of all cells without completely distinct properties. There is a significant overlap between cells with positive and negative rejuvenation index (Fig S5 and S6).

In particular, we correlated the health span to the number of divisions to investigate if rejuvenated cells have a longer life with lower damage (Fig S5A). In all cases, highly rejuvenated cells exhibit comparably large replicative lifespans. Without retention a high rejuvenation index likely also corresponds to a long health span independent of the repair mechanism. Active retention of damage leads to a qualitative difference between the repair capacities. While rejuvenated cell with unlimited repair capacity tend to have short health spans, there is no difference in health spans between cells with decline in repair capacity.

We further correlated the mean generation time of each cell to its size increase per cell cycle to see if rejuvenated cells exhibit different growth behaviour (Fig S5B). In all cases, rejuvenating cells grow comparably little in size per cell cycle. Without retention, cells with large positive rejuvenation index likely have short generation times. With retention the two repair capacities again differ. Unlimited repair capacity correlates long generation times with rejuvenation. In contrast, decline in repair capacity shows again no correlation.

These results suggest that it is in general not possible to predict rejuvenation

from single-cell properties disregarding the lineage position. However, there are visible trends for predicting properties given that the cell rejuvenates, that are moreover influenced by the repair profiles in case of active damage retention.

Effect of stress on rejuvenation and health

Lastly, we investigated how cell populations are affected by stress (Fig 5) by increasing the damage formation rate k_1 . Due to accelerated damage formation cells divide fewer times and the populations do not reach the same size in all cases. Rejuvenation can still be observed in the same manner as in *wildtype* cells: mostly cells that come from old grandmothers and comparably young mothers are prone to rejuvenation. The health span is not affected by stress with retention. However, without retention old and damaged grandmothers lead to shorter health spans of their progeny in the second generation.

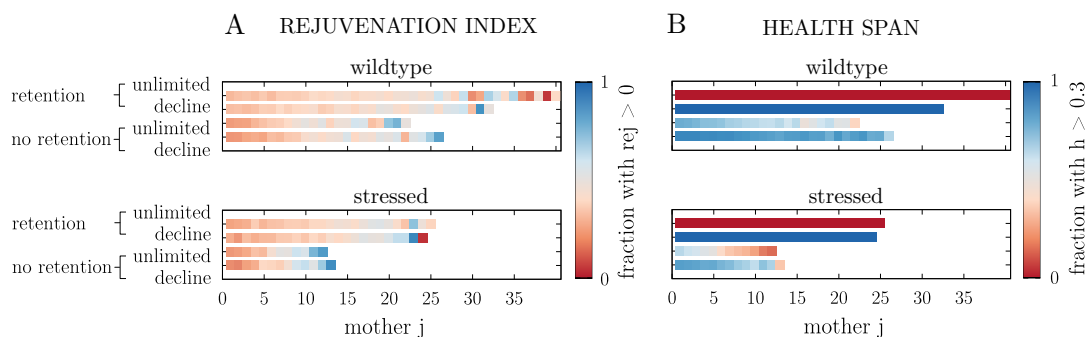


Figure 5: Effect of stress on (A) the rejuvenation index and (B) the health span in *wildtype* populations. Cells are grouped according to their lineage position j . Each population is initialised with 10 independent founder cells with average initial conditions and parameters according to SI S3. Stress corresponds to an increase in the damage formation rate by 1%.

Discussion

Starting from a theoretical description of damage accumulation in a single cell, we have developed a holistic model of replicative ageing on the population level. By defining novel features on the population level such as the health span and the rejuvenation index in addition to previously known metrics such as the replicative life span, growth per cell cycle and cumulative growth, we characterise the precise large scale impact of single-cell properties on the lineage. More precisely, we conclude that investing in an efficient repair machinery early in life followed

by a steep decline in the capacity to repair later generates longer health spans compared to having a constant repair capacity throughout the lifespan. Further, we show that retention of damage, which is detrimental to individual mother cells, reduces the variability in damage levels over generations and increases the average replicative lifespan of the population. Thus, using this framework we can concertise vague terms such as healthy ageing and test evolutionary hypotheses that are otherwise hard to quantify.

Currently, a popular notion in medicine focusing on humans is what is known as healthy ageing. Partly, this broad term focuses on a overall good quality of life of older people [47]. Based on this concept, we defined the health span h (Box 1) being a quantifiable unicellular metric based on the proportion of an individual cell's life that it remains healthy. In this context, healthy denotes that the intracellular damage levels are below a critical threshold value, i.e. $D < D_c$, such that large values of h imply that the cell spent a large proportion of its life with low damage levels and a small proportion of its life with high damage levels. In addition to this metric, we calculate other properties such as the rejuvenation index, the growth per cell cycle and the cumulative growth, which combined with the individuality of the cells reflected in the rate parameters (Eq 2) constitute a computational setup for analysing ageing on a population level. Using this novel and forceful framework, we can quantify the effect of altering intracellular properties, such as the capacity to repair damage, on the accumulation of damage for entire populations as well as individual cells.

Previously, the importance of an efficient repair machinery has been stressed [43, 44] which lead us to investigate a biologically reasonable repair profile. It is based on the assumption that the capacity to repair damage, in similarity to most other intracellular systems, declines with age. To this end, we introduced a novel repair profile (Fig 2) which invests in repair early in life while no damage is repaired late in life. This was compared to a constant repair capacity throughout the life span of a single cell. A declining capacity to repair damage is not only biologically justifiable but we could show that it is even beneficial for the individual cell as it results in lower generation times and larger health spans compared to the constant counterpart, and in fact this also holds on the population level (Fig 3 and Fig 4). This can be explained by the fact that more damage is cleared early in life leading to more divisions when the cell has low intracellular levels of damage, while no damage is repaired late in life resulting in the cell spending a small proportion of its life with high damage levels before undergoing senescence.

Moreover, one of the strengths of the model is that it is not merely restricted to the analysis of individual cells as it has the possibility to extrapolate from the single cell to the population level. With respect to the major metrics of ageing, we showed that retention of damage decreases the variability on the population level. For instance, when studying the rejuvenation index, the replicative lifespan and

the health span it is clear that the populations with retention have less variance compared to the counterparts without (Fig 4). This implies that the fate of the daughter cells in populations with retention is more similar to that of their mothers compared to the populations without retention, where for example some cells have very long replicative lifespans while others have very short ones. The fact that the daughters are more similar to their respective mothers in population with retention implies that later branches in the pedigree are more likely to survive which not only increases the overall replicative age but also the size of the population (Fig 3).

A relevant question to pose is, under what circumstances is it beneficial and disadvantageous respectively for the progenitor cells to retain damage? In harsh environments characterised by highly variable conditions cells die from other factors than ageing [1], suggesting it could be advantageous to have a few cells with high fitness which would argue in favour of cells not retaining damage. However, in more stable environments where food is more plentiful retention of damage could be beneficial as populations become bigger and the average fitness is higher. Moreover, this would suggest that ageing has evolved as a consequence of organisms moving to nutrient rich conditions with little stress.

Methods

All simulations and the analysis were performed in the programming language Julia [48] and were run on a computer with an Intel(R) Xeon(R) Platinum 8180 CPU @ 2.50GHz and Julia version 1.1. The developed model can be downloaded from github <https://github.com/cvijoviclab/RejuvenationProject>. Model parameters, constraints and relevant pseudo code for creating lineages can be found in the supplementary.

Acknowledgements

This work was supported by Swedish Agency for Strategic Research (Grant Nr. FFL15-0238 and IB13-0022). We would like to thank all past and present members of the CvijovicLab for valuable input and careful reading of the manuscript.

References

- (1) Carnes, B. A.; Nakasato, Y. R.; Olshansky, S. J. *Ageing Horizons* **2005**, *3*, 22–27.
- (2) Gavrilov, L. A.; Gavrilova, N. S. *The Scientific World Journal* **2002**, *2*, 339–356.
- (3) Kirkwood, T. B. L. *Nature* **1977**, *270*, 301–304.
- (4) Nystrom, T. *Philosophical Transactions of the Royal Society B: Biological Sciences* **2011**, *366*, 71–75.
- (5) Limpert, E. et al. *Cell reports* **2014**, *127*, 40–48.
- (6) Nyström, T.; Liu, B. *Current Opinion in Microbiology* **2014**, *18*, 61–67.
- (7) McClellan, A. J.; Tam, S.; Kaganovich, D.; Frydman, J. *Nature Cell Biology* **2005**, *7*, 736–741.
- (8) Chen, B.; Retzlaff, M.; Roos, T.; Frydman, J. *Cold Spring Harbor Perspectives in Biology* **2011**, *3*, 1–14.
- (9) Vilchez, D.; Saez, I.; Dillin, A. *Nature Communications* **2014**, *5*, 1–13.
- (10) Santra, M.; Dill, K. A.; De Graff, A. M. *Proceedings of the National Academy of Sciences of the United States of America* **2019**, *116*, 22173–22178.
- (11) Laun, P.; Pichova, A.; Madeo, F.; Fuchs, J.; Ellinger, A.; Kohlwein, S.; Dawes, I.; Fröhlich, K. U.; Breitenbach, M. *Molecular Microbiology* **2001**, *39*, 1166–1173.
- (12) Levine, R. L. *Free Radical Biology and Medicine* **2002**, *32*, 790–796.
- (13) Liu, B.; Larsson, L.; Franssens, V.; Hao, X.; Hill, S. M.; Andersson, V.; Höglund, D.; Song, J.; Yang, X.; Öling, D.; Grantham, J.; Winderickx, J.; Nyström, T. *Cell* **2011**, *147*, 959–961.
- (14) Ackermann, M.; Stearns, S. C.; Jenal, U. *Science* **2003**, *300*, 1920.
- (15) Stewart, E. J.; Madden, R.; Paul, G.; Taddei, F. *PLoS Biology* **2005**, *3*, 0295–0300.
- (16) Rujano, M. A.; Bosveld, F.; Salomons, F. A.; Dijk, F.; Van Waarde, M. A.; Van Der Want, J. J.; De Vos, R. A.; Brunt, E. R.; Sibon, O. C.; Kampinga, H. H. *PLoS Biology* **2006**, *4*, 2325–2335.
- (17) Nyström, T. *PLoS Genetics* **2007**, *3*, 2355–2357.
- (18) Lindner, A. B.; Madden, R.; Demarez, A.; Stewart, E. J.; Taddei, F. *Proceedings of the National Academy of Sciences* **2008**, *105*, 3076–3081.

- (19) Fuentealba, L.; Eivers, E.; Geissert, D.; Taelman, V.; De Robertis, E. M. *Chemtracts* **2008**, *21*, 119–120.
- (20) Bufalino, M. R.; DeVeale, B.; van der Kooy, D. *Journal of Cell Biology* **2013**, *201*, 523–530.
- (21) Hernebring, M.; Fredriksson, Å.; Liljevald, M.; Cvijovic, M.; Norrman, K.; Wiseman, J.; Semb, H.; Nyström, T. *Scientific Reports* **2013**, *3*, 1–6.
- (22) Ogrodnik, M.; Salmonowicz, H.; Brown, R.; Turkowska, J.; Sredniawa, W.; Pattabiraman, S.; Amen, T.; Abraham, A. C.; Eichler, N.; Lyakhovetsky, R.; Kaganovich, D. *Proceedings of the National Academy of Sciences of the United States of America* **2014**, *111*, 8049–8054.
- (23) Ackermann, M.; Chao, L.; Bergstrom, C. T.; Doebeli, M. *Aging Cell* **2007**, *6*, 235–244.
- (24) Wang, X.; Tsai, J. W.; Imai, J. H.; Lian, W. N.; Vallee, R. B.; Shi, S. H. *Nature* **2009**, *461*, 947–955.
- (25) Oliaro, J. et al. *The Journal of Immunology* **2010**, *185*, 367–375.
- (26) Egilmez, N. K.; Jazwinski, S. M. *Journal of bacteriology* **1989**, *171*, 37–42.
- (27) Aguilaniu, H.; Gustafsson, L.; Rigoulet, M.; Nyström, T. *Science* **2003**, *299*, 1751–1753.
- (28) Henderson, K. A.; Gottschling, D. E. *Current Opinion in Cell Biology* **2008**, *20*, 723–728.
- (29) Mortimer, R. K.; Johnston, J. R. *Nature* **1959**, *183*, 1751–1752.
- (30) Steinkraus, K.; Kaeberlein, M.; Kennedy, B. *Annual Review of Cell and Developmental Biology* **2008**, *24*, 29–54.
- (31) Longo, V. D.; Shadel, G. S.; Kaeberlein, M.; Kennedy, B. *Cell Metabolism* **2012**, *16*, 18–31.
- (32) He, C.; Zhou, C.; Kennedy, B. K. *Biochimica et Biophysica Acta - Molecular Basis of Disease* **2018**, *1864*, 2690–2696.
- (33) Erjavec, N.; Larsson, L.; Grantham, J.; Nyström, T. *Genes and Development* **2007**, *21*, 2410–2421.
- (34) Liu, B.; Larsson, L.; Caballero, A.; Hao, X.; Öling, D.; Grantham, J.; Nyström, T. *Cell* **2010**, *140*, 257–267.
- (35) Coelho, M.; Tolić, I. M. *BioEssays* **2015**, *37*, 740–747.
- (36) Kennedy, B. K.; Austriaco, N. R.; Guarente, L. *Journal of Cell Biology* **1994**, *127*, 1985–1993.

- (37) Sinclair, D. A.; Mills, K.; Guarente, L. *Trends in Biochemical Sciences* **1998**, *23*, 131–134.
- (38) Chao, L. *PLoS Genetics* **2010**, *6*, DOI: 10.1371/journal.pgen.1001076.
- (39) Erjavec, N.; Cvijovic, M.; Klipp, E.; Nystrom, T. *Proceedings of the National Academy of Sciences* **2008**, *105*, 18764–18769.
- (40) Rashidi, A.; Kirkwood, T. B.; Shanley, D. P. In *Subcellular Biochemistry, Aging Research in Yeast*; Springer-Verlag: 2012; Vol. 57, pp 315–331.
- (41) Vedel, S.; Nunns, H.; Košmrlj, A.; Semsey, S.; Trusina, A. *Cell Systems* **2016**, *3*, 187–198.
- (42) Borgqvist, J.; Welkenh, N.; Cvijovic, M. *Scientific Reports* **2020**, *10*, 1–14.
- (43) Clegg, R. J.; Dyson, R. J.; Kreft, J. U. *BMC Biology* **2014**, *12*, DOI: 10.1186/s12915-014-0052-x.
- (44) Song, R.; Acar, M. *BMC Bioinformatics* **2019**, *20*, 1–14.
- (45) Karlsson, M.; Janzén, D. L.; Durrieu, L.; Colman-Lerner, A.; Kjellsson, M. C.; Cedersund, G. *BMC Systems Biology* **2015**, *9*, 1–15.
- (46) Liu, P.; Acar, M. *Science Advances* **2018**, *4*, 1–9.
- (47) Peel, N.; Bartlett, H.; McClure, R. *Australasian Journal on Ageing* **2004**, *23*, 115–119.
- (48) Bezanson, J.; Edelman, A.; Karpinski, S.; Shah, V. B. *SIAM Review* **2017**, *59*, 65–98.

The Synergy of Damage Repair and Retention Promotes Rejuvenation and Prolongs Healthy Lifespans in Cell Lineages

Supplementary Information (SI)

Barbara Schnitzer ¹, Johannes Borgqvist ¹, Marija Cvijovic ^{1*}

¹ Department of Mathematical Sciences, University of Gothenburg, Sweden

* corresponding author: Marija Cvijovic, marija.cvijovic@chalmers.se

Contents

S1 Non-dimensionalisation of the model	i
S2 The repair term with the repair capacity R	ii
S3 Practical aspects	iii
S3.1 Fixed parameters and conventions	iii
S3.2 Create lineage	iii
S3.3 Finding <i>wildtype</i> cells in the parameter space	iv
S3.4 Average initial conditions in a cell lineage	vi
S4 Gradients of the rate parameters for maintaining constant replicative lifespan	vii
S5 Effect of the definition of health span and the choice of the threshold	vii
S6 Complementing properties of <i>wildtype</i> cell populations	ix

S1 Non-dimensionalisation of the model

model	original	non-dimensionalised
$\dot{P}(t)$	$\mu P(t) \left(g - \frac{D(t)}{D_c} \right)$ $- k_1 P(t)$ $+ \frac{k_2 R}{\pi} \sin \left[\frac{\pi}{R} \frac{D(t)}{D_c} \right]$	$P(t) (g - D(t))$ $- k_1 P(t)$ $+ k_2 R Q \sin \left[\frac{D(t)}{R} \right]$
$\dot{D}(t)$	$+ k_1 P(t)$ $- \frac{k_2 R}{\pi} \sin \left[\frac{\pi}{R} \frac{D(t)}{D_c} \right]$	$+ \frac{k_1}{Q} P(t)$ $- k_2 R \sin \left[\frac{D(t)}{R} \right]$
parameter bounds	$P \in [0, P_c], \quad D \in [0, D_c]$ $g \geq 1, \quad \mu, k_1, k_2 > 0$ $R \geq 1$	$P \in [0, 1], \quad D \in [0, 1]$ $g \geq 1, \quad k_1, k_2 > 0$ $R \geq \pi^{-1}$
content at division in mother :		
intact P	$s P_c - re(1-s)D$	$s - re(1-s)QD$
damaged D	$sD + re(1-s)D$	$sD + re(1-s)D$
in daughter :		
intact P	$(1-s)P_c + re(1-s)D$	$(1-s) + re(1-s)QD$
damaged D	$(1-s)D - re(1-s)D$	$(1-s)D - re(1-s)D$
# parameters	7	5

Table S1: Comparison between the model before and after non-dimensionalisation.

One can reduce the complexity of the system by rescaling its variables and parameters without changing the qualitative behaviour. The right column of Table S1 is obtained by dividing the equation for $\dot{P}(t)$ by μP_c , respectively $\dot{D}(t)$ by μD_c , and updating the parameters definitions. In particular, we update $t \leftarrow \mu t$, $P \leftarrow \frac{P}{P_c}$, $D \leftarrow \frac{D}{D_c}$, $Q \leftarrow \frac{D_c}{P_c}$, $k_1 \leftarrow \frac{k_1}{\mu}$, $k_2 \leftarrow \frac{k_2}{\mu D_c}$ and $R \leftarrow \frac{R}{\pi}$. The distribution of the protein content at division is altered analogously. As a result, the overall parameter space reduces from 7 to 5 dimensions.

S2 The repair term with the repair capacity R

The essential part of the repair term in the single-cell ODE model is

$$r(D) = k_2 R \sin \left[\frac{D(t)}{R} \right].$$

We use a scaled sine function to incorporate the repair capacity. It should not be connected to any oscillatory behaviour since only maximally half a period is captured by the model due to the bounds on $P(t) \in [0, 1]$, $D(t) \in [0, 1]$ and $R \in [\pi^{-1}, \infty]$. R changes the period length of the sine and so tunes how much the repair declines with increasing D . As R approaches infinity $\sin \left[\frac{D(t)}{R} \right] \approx \frac{D(t)}{R}$ and the repair velocity becomes a linear function as in [42]. It is equivalent to a very large period length of the sine function. Decreasing R will continuously decrease the period length and eventually when $R = \pi^{-1}$ the repair will decline all the way to 0 again at the cell's maximal damage level $D(t) = 1$. Only in this extreme case exactly half a period of the sine is captured. In all other cases it is less than half a period.

Since the sine function is linear for small arguments, the behaviour for small amounts of damage ($D \rightarrow 0$) is the same for all values of R . In particular, the rate of repair in that regime corresponds to k_2 . However, the profiles differ increasingly while ageing (Fig 2).

The repair term in our model is not derived from first principles and does not explain mechanistic details of the repair machinery, but only helps to understand the consequences of a specific profile. Instead of creating several models there is an extra tunable parameter R , which compresses and simplifies the analysis of the model.

S3 Practical aspects

S3.1 Fixed parameters and conventions

name	parameter	value
size proportion	s	0.6370
damage resilience	Q	2.5526
growth factor	g	1.05
random effects in rate parameters	σ	0.005
no retention $\hat{=}$ damage in mother at division	re	0.0 63.70%
retention $\hat{=}$ damage in mother at division	re	0.2957 74.43%
unlimited repair capacity	R	10^3
decline in repair capacity	R	π^{-1}
maximal generation in lineage		3
critical threshold defining the health span	D_c	0.5
threshold for healthy cells	h_c	0.3

Table S2: Fixed parameters and conventions used in the paper.

The size proportion, damage resilience, growth factor and the maximal retention factor were estimated in [42].

S3.2 Create lineage

In most simulations we generate lineages up to 3 generations. The ODEs of a cell are not coupled to any other cell. Therefore, each cell can be solved individually. In case there is some coupling between the cells, e.g. time or shared food resources, all ODEs of alive cells have to be solved at the same time instead and dead cells have to be removed from the system.

Algorithm 1 Create lineage (uncoupled cells)

```
1: Define all relevant parameters
2: Initialise  $n$  founder cell(s) with identifiers  $1, \dots, n$ 
3: Set (dynamic) lineage size  $N \leftarrow n$ 
4: Set maximal generation number  $M$ 
5:
6: for  $i \in 1..N$  do
7:   while true do
8:     Solve ODE of cell  $i$  until it divides ( $P(t) = 1$ ) or dies ( $D(t) = 1$ )
9:     Keep track of all wanted properties
10:    if  $P(t) = 1$  then
11:      Reset protein content of mother cell according to division rules
12:    else if  $D(t) = 1$  then
13:      break
14:    end if
15:  end while
16:
17:  if daughters are in generation  $m < M$  then
18:    Add  $rls$  new daughter cells to the lineage according to division rules with
    identifiers  $N + 1, \dots, N + rls$ 
19:     $N \leftarrow N + rls$ 
20:  end if
21: end for
22:
23: Save all wanted information
24: Analyse population properties
```

S3.3 Finding *wildtype* cells in the parameter space

In order to find parameter combinations in the k_1 , k_2 and re space that lead to 24 divisions we use an iterative process with adaptive step size. Typically, we fix two of the three dimensions to a value and find the third one. Algorithm 2 shows an example for adapting k_2 if all other parameters are set.

Algorithm 2 Finding *wildtype* cells

```
1: Define all relevant parameters
2: Set initial conditions of cell to  $P(0) = 1 - s$ ,  $D(0) = 0$ 
3: Set wanted replicative lifespan  $rls^* = 24$ 
4: Set initial value of the parameter to adapt  $k_2 = 0$ 
5: Set initial step size  $\Delta k_2$  and minimal step size  $\Delta k_2 \geq \delta$ 
6:
7: Coarse search :
8: while true do
9:    $k_2 \leftarrow k_2 + \Delta k_2$ 
10:  Run single-cell model
11:  if ( $rls > rls^*$ ) then
12:    break
13:  end if
14: end while
15:
16: Fine search with adaptive step size :
17: while true do
18:   $\Delta k_2 \leftarrow \Delta k_2 \cdot 0.5$ 
19:  Run single-cell model
20:  if ( $rls == rls^*$  or  $\Delta k_2 < \delta$ ) then
21:    break
22:  else if  $rls > rls^*$  then
23:     $k_2 \leftarrow k_2 - \Delta k_2$ 
24:  else
25:     $k_2 \leftarrow k_2 + \Delta k_2$ 
26:  end if
27: end while
28:
29: wildtype is found if  $rls == rls^*$  and the corresponding parameter is  $k_2$ 
```

In the same manner, one can start with many cells and allow for parameter variations in k_1 and k_2 according to non-linear mixed effects (equation (2)) and check if the average value of the respective parameter is around the wanted replicative lifespan with some tolerance. The algorithm does not necessarily have to be 24 as it is for the *wildtype* yeast cells, but works for any preset replicative lifespan. Note that when varying the retention factor, it is computationally more efficient to start from a high value and reduce it stepwise. Corresponding signs have to be adapted.

In the paper we often compare four cases, which correspond to following

parameter combinations.

repair mechanism	retention	$(re, \bar{k}_1, \bar{k}_2, R)$
unlimited repair capacity	retention	$(0.2957, 0.4, 0.09219, 10^3)$
	no retention	$(0.0, 0.4, 0.02438, 10^3)$
decline in repair capacity	retention	$(0.2957, 0.4, 0.13750, \pi^{-1})$
	no retention	$(0.0, 0.4, 0.03125, \pi^{-1})$

Table S3: Parameter combinations for *wildtype* populations.

S3.4 Average initial conditions in a cell lineage

For all population studies the founder cells start with initial conditions $\bar{P}(0)$ and $\bar{D}(0)$ which are specific to a set of parameters. Starting with an average cell gives rise to more realistic populations and facilitates the analysis since it is not necessary to simulate a large amount of generations to get a representative view on the populations. The initial conditions are found according to algorithm 3. The algorithm converges independent of the age of the founder cell up to a certain precision. With $\epsilon = 10^{-3}$ no numerical issues were faced and the values are sufficiently precise for our purpose.

Algorithm 3 Finding average initial conditions

```

1: Define all relevant parameters
2: Set initial conditions of founder cell to  $P(0) = 1 - s$ ,  $D(0) = 0$ 
3: Set tolerance  $\epsilon$ 
4:
5: while true do
6:   Create founder cell with  $P(0)$  and  $D(0)$ 
7:   Run population model and obtain lineage
8:    $\bar{P}(0) \leftarrow$  average intact protein content at birth in lineage
9:    $\bar{D}(0) \leftarrow$  average damaged protein content at birth in lineage
10:  if  $(|\bar{P}(0) - P(0)| \leq \epsilon$  and  $|\bar{D}(0) - D(0)| \leq \epsilon)$  then
11:    break
12:  else
13:     $P(0) \leftarrow \bar{P}(0)$ 
14:     $D(0) \leftarrow \bar{D}(0)$ 
15:  end if
16: end while
17:
18:  $\bar{P}(0)$  and  $\bar{D}(0)$  are the average initial conditions

```

S4 Gradients of the rate parameters for maintaining constant replicative lifespan

We estimate the gradients on the parameter surface determining *wildtype* cells (Fig 2) for constant k_1 , k_2 or re by linearly approximating how much the other two parameters have to be changed in order to stay on the surface.

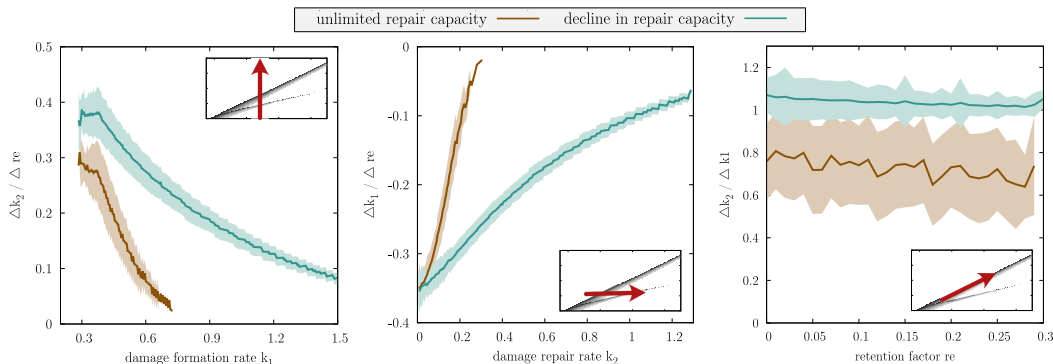


Figure S1: Estimated gradients for *wildtype* cells in the k_1 , k_2 and re space (Fig 2). We approximate a linear change in all directions between points on the grid and show the mean and standard deviation of the change in a certain direction (marked by red arrow in parameter space).

S5 Effect of the definition of health span and the choice of the threshold

The threshold for the health span is more or less arbitrarily chosen as $D_c = 0.5$. Too high and too low values are not reasonable to take, since then all cells have either health span of $h \approx 1$ or $h \approx 0$ respectively. For an intermediate threshold we can however observe differences between the repair capacities (Figure S2). The qualitative conclusions are the same independent of the choice of D_c if not too close to the extremes such that 0.5 seems to be a valid compromise.

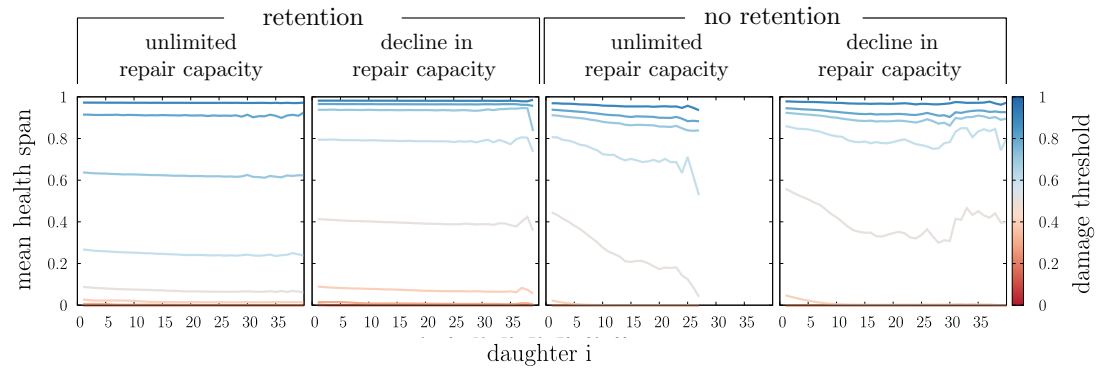


Figure S2: Mean health span as a function of the lineage position i . Each population is initialised with 10 independent founder cells with average initial conditions and parameters according to SI S3.

S6 Complementing properties of *wildtype* cell populations

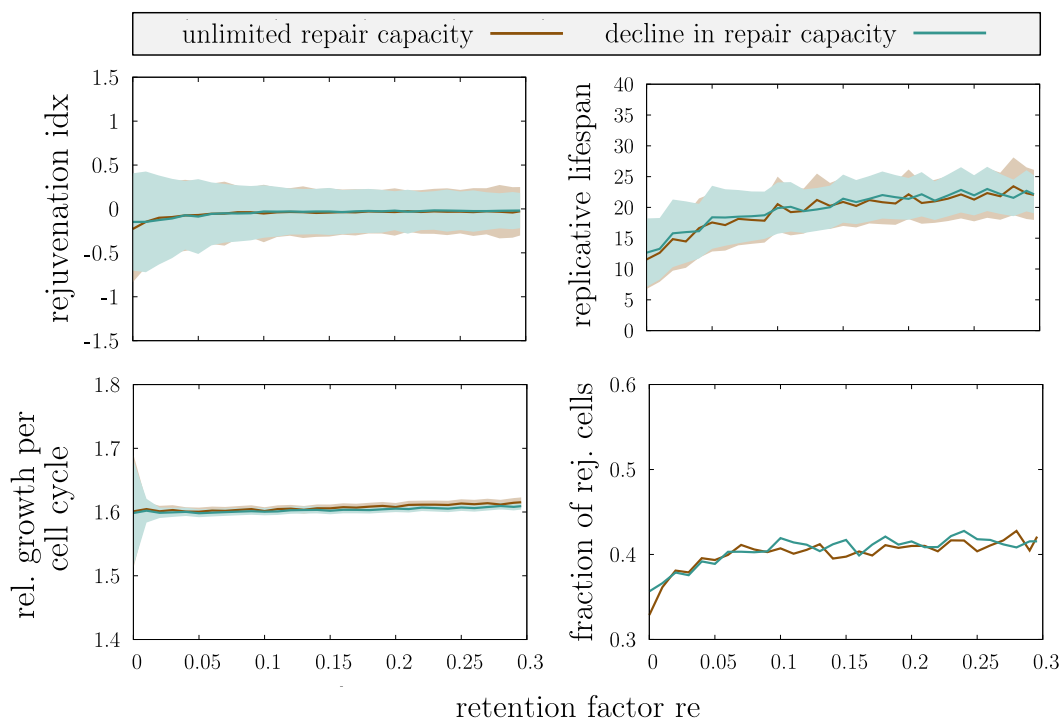


Figure S3: Mean and standard deviation or fraction of single-cell properties in *wildtype* cell lineages for varying retention factors re . Each population is initialised with 5 independent founder cells with average initial conditions and parameters according to SI S3.

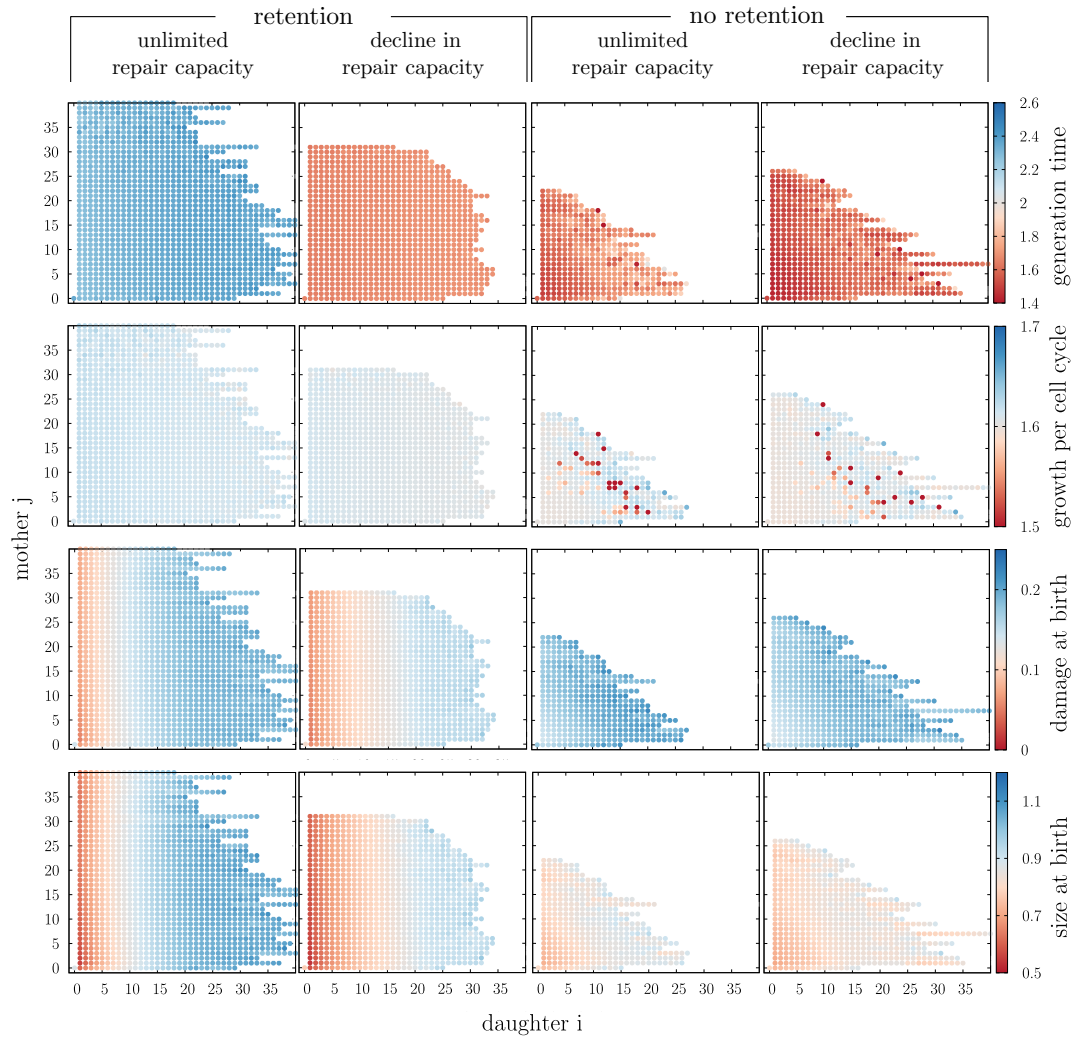


Figure S4: Mean of single-cell properties for *wildtype* cells that have the same lineage position with respect to the grandmother (indices i and j in lineage position). The analysed population is the same as in Figure 4.

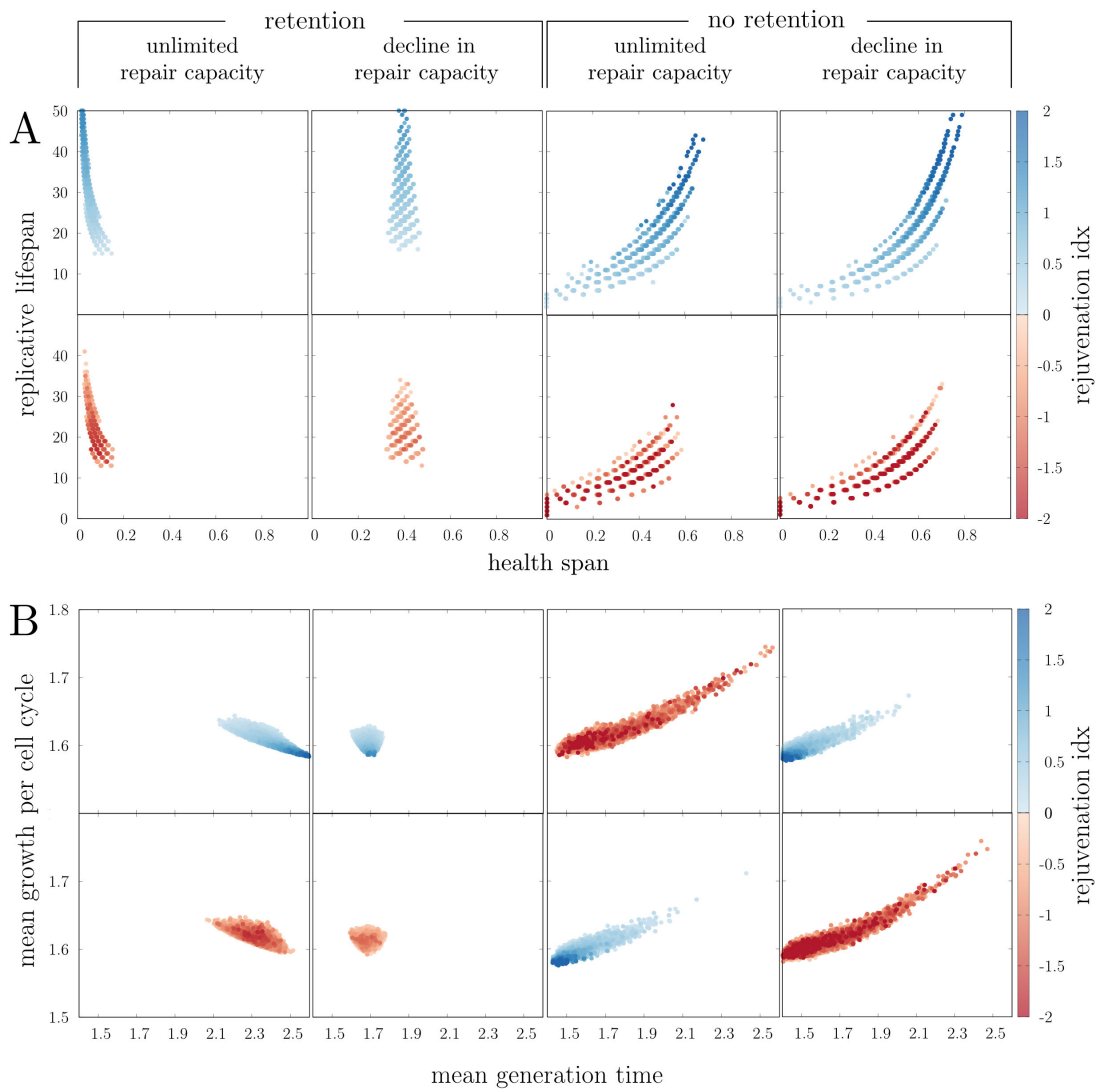


Figure S5: Correlation between single-cell properties in *wildtype* populations with focus on rejuvenated cells. Each point corresponds to a cell in the lineage. Points can lie on top of each other. The analysed population is the same as in Figure 4.

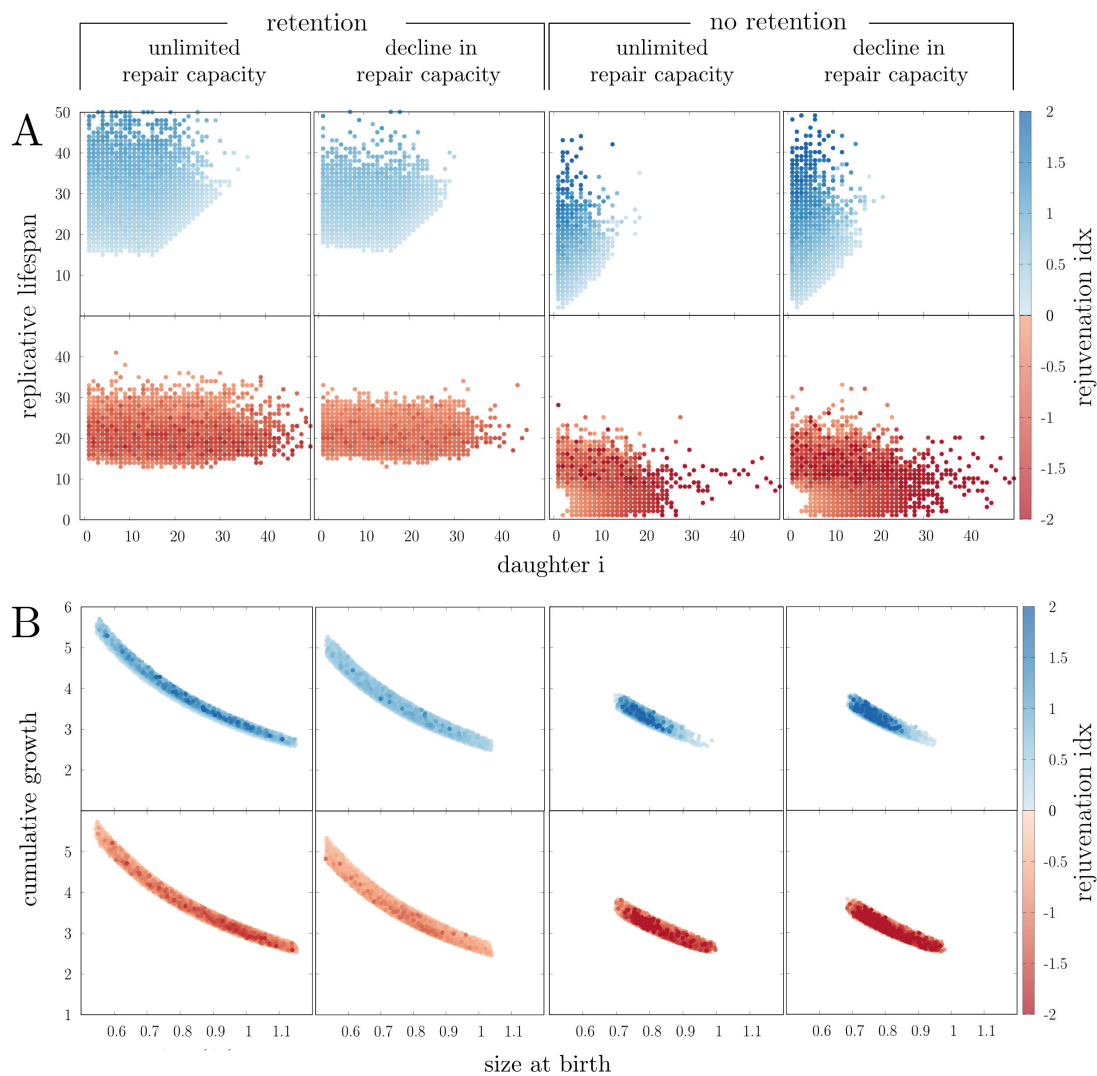


Figure S6: Correlation between single-cell properties in *wildtype* populations with focus on rejuvenated cells. Each point corresponds to a cell in the lineage. Points can lie on top of each other. The analysed population is the same as in Figure 4.